Solar Energy Materials and Solar Cells 183 (2018) 164–172

Contents lists available at ScienceDirect

Solar Energy Materials and Solar Cells

journal homepage: www.elsevier.com/locate/solmat

Superacid-derived surface passivation for measurement of ultra-long lifetimes in silicon photovoltaic materials

A.I. Pointon[a], N.E. Grant[a], E.C. Wheeler-Jones[b], P.P. Altermatt[c], J.D. Murphy[a,*]

[a] School of Engineering, University of Warwick, Coventry CV4 7AL, United Kingdom
[b] Department of Chemistry, University of Warwick, Coventry CV4 7AL, United Kingdom
[c] Trina Solar Limited, Changzhou 213031, China

ARTICLE INFO

Keywords:
Silicon
Surface
Passivation
Lifetime
Superacid

ABSTRACT

Accurate measurements of bulk minority carrier lifetime are essential in order to determine the true limit of silicon's performance and to improve solar cell production processes. The thin film which forms when silicon wafers are dipped in solutions containing superacids such as bis(trifluoromethane)sulfonimide (TFSI) has recently been found to be effective at electronically passivating the silicon surface. In this paper we first study the role of the solvent in which TFSI is dissolved for the passivation process. We study ten solvents with a wide range of relative polarities, finding TFSI dissolved in hexane provides improved temporal stability, marginally better passivation and improved solution longevity compared to dichloroethane which has been used previously. Sample storage conditions, particularly humidity, can strongly influence the passivation stability. The optimised TFSI-hexane passivation scheme is then applied to a set of 3 Ω cm *n*-type wafers cut from the same float-zone ingot to have different thicknesses. This enables the reproducibility of the scheme to be systematically evaluated. At 10^{15} cm^{-3} injection the best case effective surface recombination velocity is 0.69 ± 0.04 cm/s, with bulk lifetimes measured up to the intrinsic lifetime limit at high injection and > 43 ms at lower injection. Immersion of silicon in superacid-based ionic solutions therefore provides excellent surface passivation, and, as it is applied at room temperature, the effects on true bulk lifetime are minimal.

1. Introduction

The highest efficiency silicon solar cells require substrates with bulk minority carrier lifetimes well into the millisecond range. Recent advances in wafer production and processing technologies mean that the true lifetime limit is not known, with several recent studies [1–5] reporting lifetimes higher than the currently accepted intrinsic “limit” due to Auger and radiative recombination [6].

To measure high bulk lifetimes accurately, it is necessary to have excellent surface passivation to minimise recombination at the surface. Dielectric-based surface passivation (see Ref. [7] for a review) can provide excellent stable passivation, although the passivation process itself can affect the bulk lifetime due to bulk passivation, external gettering [8] or thermal effects. These artefacts can often be avoided if room temperature temporary surface passivation is used instead, and this has been recently reviewed by Grant and Murphy [9]. Temporary passivation has traditionally been achieved by immersion of samples in solutions of acids, halogen-alcohols or benzyl-alcohols, but such liquid-based methods are not easy to characterise using conventional approaches. Recently a new class of temporary passivation has been developed, whereby a thin film is formed when silicon samples are treated with a superacid-containing solution at room temperature [2,10]. When the surface pre-treatment and processing are optimised, it has been shown that the resulting effective surface recombination velocity is below 1 cm/s [2]. Thus, the level of passivation is similar to some of the best dielectric-schemes, but possible changes in bulk lifetime during the passivation step are avoided due to the low temperatures used. This passivation scheme can therefore be used to measure true bulk lifetimes resulting from cell processing, as recently done in the fabrication of interdigitated back contact (IBC) solar cells [11].

The initial work by Bullock et al. examined various superacid solutions finding bis(trifluoromethane)sulfonimide (TFSI) crystals dissolved in 1,2-dichloroethane (DCE) to give the best surface passivation [10]. This composition was taken forward by Grant et al., who optimised the surface pre-treatments, and demonstrated the measurement of extremely high lifetimes (up to 75 ms) in high resistivity silicon [2]. However, there are now good reasons to re-examine the composition of the ionic solution used in the passivation process. First, DCE is classified as “possibly carcinogenic to humans” by the World Health Organization [12] so may be best avoided. Second, by changing the composition of

* Corresponding author.
E-mail address: john.d.murphy@warwick.ac.uk (J.D. Murphy).

https://doi.org/10.1016/j.solmat.2018.03.028
Received 13 February 2018; Accepted 14 March 2018
Available online 26 April 2018

Table 1
Solvents for TFSI investigated in this study. All solvents are in anhydrous forms. Relative polarities are taken from Ref. [19].

Label	Solvent name used	Chemical name	Formula	Relative polarity	Supplier (product number)	Purity
A	Acetone	2-propanone	C_3H_6O	0.355	VWR (83683)	99.9%
B	Chlorobenzene	Chlorobenzene	C_6H_5Cl	0.188	Sigma Aldrich (284513)	99.8%
C	Cyclohexane	Cyclohexane	C_6H_{12}	0.006	Sigma Aldrich (227048)	99.5%
D	Dichloroethane (DCE)	1,2-dichloroethane	$C_2H_4Cl_2$	0.327	Sigma Aldrich (284505)	99.8%
E	Dioxane	1,4-dioxane	$C_4H_8O_2$	0.164	Sigma Aldrich (296309)	99.8%
F	Dichloromethane (DCM)	Dichloromethane	CH_2Cl_2	0.309	Alfa Aesar (41835)	99.7%
G	Hexane	*n*-hexane	C_6H_{14}	0.009	Sigma Aldrich (296090)	95%
H	Isopropanol (IPA)	2-propanol	C_3H_8O	0.546	Sigma Aldrich (278475)	99.5%
I	Octane	*n*-octane	C_8H_{18}	0.012	Sigma Aldrich (296988)	> 99%
J	Toluene	Toluene	C_7H_8	0.099	Sigma Aldrich (244511)	99.8%

the solution it may be possible to improve its long-term stability, and this may be important in converting what is currently a temporary passivation scheme into a more permanent one. Third, the mechanism by which the thin film passivates the silicon surface is not currently clear, and understanding the effect of varying the solvent may improve fundamental understanding. This has implications beyond silicon-based photovoltaics, as TFSI-containing electrolytes are being studied as a potential way to stabilise silicon-based anodes for lithium ion batteries [13].

This paper reports the results of an investigation to develop alternative ionic solutions for surface passivation, which do not rely on DCE. A series of experiments is performed to passivate silicon wafer surfaces with TFSI dissolved in different solvents which have a wide range of relative polarities. The passivation effects are quantified using carrier lifetime measurements and the temporal stability is studied taking into account variables such as solution age and the humidity of sample storage between measurements. The effective surface recombination velocity and bulk lifetime are extracted by using a robust method involving variable thickness samples cut from the same high purity ingot. Finally, we report the results of a series of tests to assess the reproducibility of the optimal process.

2. Experimental methods

2.1. Samples and surface preparation

Most experiments were performed on quarters of 5 Ω cm *n*-type (100) orientation 100 mm diameter float-zone (FZ) silicon wafers with an initial thickness of 750 μm. Some experiments were performed on whole 3 Ω cm *n*-type (100) orientation 100 mm diameter FZ silicon wafers cut with a wide range of thicknesses from the same ingot. Prior to starting the passivation processes, these 3 Ω cm wafers were subjected to a 200 °C anneal for 30 min, as this has previously been found to deactivate bulk defects in FZ silicon [14–16] and for the relevant part of the study the absolute – rather than relative – lifetime is of interest. We use relatively large pieces of silicon to minimise edge effects. These can occur if the passivation film induces an inversion layer in the silicon so both carrier types can easily travel laterally to the sample's edge as majority carriers and recombine there [17,18].

All samples were subjected to a rigorous cleaning and surface preparation procedure which was developed in our previous work [2]. For all processes very high purity (18.2 MΩ) deionized (DI) water was used. Our standard procedure comprised seven stages, as follows:

1. A dip in 1% HF to remove the native oxide.
2. Standard clean 2 (SC 2), which is sometimes called RCA 2, consisting of H_2O, H_2O_2 (30%), HCl (37%) (5:1:1) for 5 min at ~75 °C.
3. A dip in 1% HF to remove the chemical oxide formed during SC 2.
4. An etch in 25% tetramethylammonium hydroxide (TMAH) for 10 min at ~80 °C.
5. A dip in 1% HF.
6. An SC 2 clean using the same chemicals as above for 10 min at ~75 °C.
7. Immersion in 2% HF for 5 s followed by air drying (no DI water rinse).

Later in this paper we conduct a series of reproducibility tests on the variable thickness 3 Ωcm wafers. After the initial complete passivation cycle and lifetime characterisation, the passivation was removed by rinsing in DI water then performing steps 1–3 above. The samples were then subjected to another 200 °C anneal for 30 min followed by steps 1–7 above again, with a slight modification so that step 4 is a 30 min TMAH etch instead.

2.2. Preparation and application of surface passivating solutions

Chemicals for passivation were measured and mixed in nitrogen (N_2) purged gloveboxes. To prepare the passivating solution, 100 mg of bis(trifluoromethane)sulfonimide (Sigma-Aldrich, 95%) crystals were measured out and then dissolved in 50 ml of an anhydrous solvent. The solvents used in this work are given in Table 1. Solvents chosen have a wide range of relative polarities with values obtained from Ref. [19]. The TFSI crystals generally dissolved in the solvents fairly rapidly, with the exception of chlorobenzene, hexane, and octane in which the crystals took several hours or even days to dissolve fully. Solutions were stored in air-tight glass bottles.

Immediately following their surface pre-treatment, as described above, silicon samples were transferred into the glovebox which was purged with N_2 to give a relative humidity below 25%. For a given treatment, a pre-prepared passivating solution was poured into a glass beaker and a silicon sample was immersed in the solution for about 60 s. The silicon sample was then removed from the passivating solution and was dried in the N_2 ambient of the glovebox. Passivated samples were then placed in plastic petri dishes and removed from the glovebox for characterisation.

2.3. Lifetime measurements

Excess carrier lifetime measurements were made using a Sinton WCT-120 photoconductance (PC) lifetime tester with an 2 cm diameter coil under transient PC mode. Care was taken always to site samples in the same place relative to the coil, and lifetimes in full wafer samples were measured at the wafer centre. Photoluminescence (PL) images were acquired with a BT Imaging LIS-L1 system to check the homogeneity of passivation. PL images were acquired with excitation by LEDs with a wavelength of 650 nm. To preserve the structural integrity of the passivating films, lifetime and PL measurements were made with the samples in the plastic petri dishes. This prevented damage occurring to the films during handling, and required recalibration of the lifetime tester to mitigate the effects of the plastic petri dish immediately above the coil. Unless otherwise stated, samples were subsequently stored in their petri dishes in the dark with their lids loosely in place between

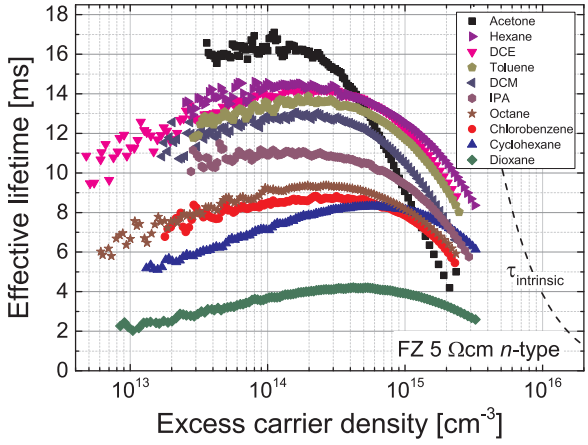

Fig. 1. Initial effective lifetime versus excess carrier density for 5 Ω cm *n*-type float-zone silicon with a thickness of 740 μm passivated with TFSI dissolved in different solvents whose properties are given in Table 1. The intrinsic lifetime limit of Richter et al. [6] is also plotted.

measurements.

The measured quantity from PC measurements is influenced by various recombination processes and is hence commonly denoted 'effected lifetime' or 'measured lifetime' and is simply denoted 'lifetime' for the rest of this paper to distinguish it from bulk lifetime. Errors in transient lifetimes were taken as ± 5%, guided by a detailed reproducibility study [20]. Where single values of lifetime are referred to in this paper they are the values at an average excess carrier concentration of 10^{15} cm^{-3} unless stated otherwise. This injection density is prevalent at the maximum power point of high-efficiency cells where the high lifetimes reported in this paper are most relevant.

3. Results

3.1. Solvent dependence

A series of experiments was performed to passivate silicon wafers with TFSI dissolved in the different solvents listed in Table 1. Fig. 1 shows the injection-dependent lifetimes measured immediately after passivation. The dependence of lifetime on excess carrier concentration is similar in character in all cases, with the exception of TFSI-acetone, TFSI-cyclohexane and possibly also TFSI-dioxane, with the last of these giving a much lower lifetime than all the other solvents studied.

Great care was taken to ensure that bulk lifetime variations which can occur between float-zone wafers within a batch [16] did not influence the results. This was done by routinely cross-checking quarter samples taken from the same wafer (hence assumed to have the same bulk lifetime) with different passivation schemes. For example, the toluene and acetone results shown in Fig. 1 were acquired from quarters taken from the same wafer, so we are sure that the different injection-dependence observed with acetone arises from the passivation and not from a bulk defect. Other pairs of samples were DCM and DCE, and chlorobenzene and octane. For other solvents cross-referencing was made to DCE as this passivation scheme was well understood from our previous work [2].

The results therefore show that the solvent has a substantial impact on the level of surface passivation achieved. There is no obvious correlation between lifetime and relative polarity as given in Table 1. For example, DCE and DCM have high relative polarities, whereas toluene and hexane have much lower relative polarities, but when used as a solvent for TFSI the lifetimes measured are similar in all cases. This is discussed later.

One of the aims of this study is to find an alternative passivation scheme to the TFSI-DCE system used previously [2,10]. The main requirement is that the alternative passivation scheme gives similarly high lifetimes, so the results presented in Fig. 1 reveal TFSI-acetone, TFSI-hexane, TFSI-toluene and TFSI-DCM as possible candidates. Whilst TFSI-acetone results in the highest lifetime in low-injection, it also causes a far stronger injection dependence than the other solvents at higher injection levels. Additionally, TFSI-acetone and TFSI-toluene passivation and their solutions are unstable, as shown later, so neither of these scheme are seen as viable TFSI-DCE alternatives.

If the superacid induces a significant amount of negative charge at the surface (discussed later), there may exist an inversion layer near the surface with a sufficiently low sheet resistivity so holes can travel to the quarter wafer sample's edge as majority carriers and recombine there. This phenomenon was reported in Ref. [18] to cause a continuous decrease in effective lifetime with decreasing injection density in low-injection. This may be the cause for our observed decrease in effective lifetime towards $\Delta n = 10^{13}$ cm^{-3}.

3.2. Degradation of passivation

A series of experiments was performed to assess the stability of the passivation achieved by TFSI dissolved in different solvents. The lifetime was measured over a one hour period and the effective lifetime is plotted as a function of time in Fig. 2, normalised by the starting lifetime. Between measurements the samples were stored in the dark in their petri dishes loosely covered by a lid. Fig. 2(a) shows the lifetime arising from TFSI dissolved in solvents shown to have a relatively high starting lifetime in Fig. 1, and Fig. 2(b) shows the results for the relatively low lifetime cases.

For the relatively high lifetime passivation schemes shown in Fig. 2(a) the lifetime is relatively stable (i.e. within 10% of the initial lifetime over 1 h) only for TFSI-toluene and TFSI-hexane. The other systems are less stable. For the relatively low lifetime cases shown in Fig. 2(b), TFSI-chlorobenzene and TFSI-cyclohexane exhibit very good stability (again within 10%), whilst TFSI-IPA, TFSI-octane and TFSI-dioxane were less stable.

In terms of TFSI-DCE replacement, the stability measurements leave only TFSI-hexane and TFSI-toluene as the remaining candidates. In contrast, TFSI-DCM passivation improves significantly with time after application which is not desirable for a reproducible measurement. Further to this, it is also desirable to avoid the use of a chlorinated solvent. We favour TFSI-hexane over TFSI-toluene as it gives slightly superior bulk lifetimes and longer solution stability as discussed later.

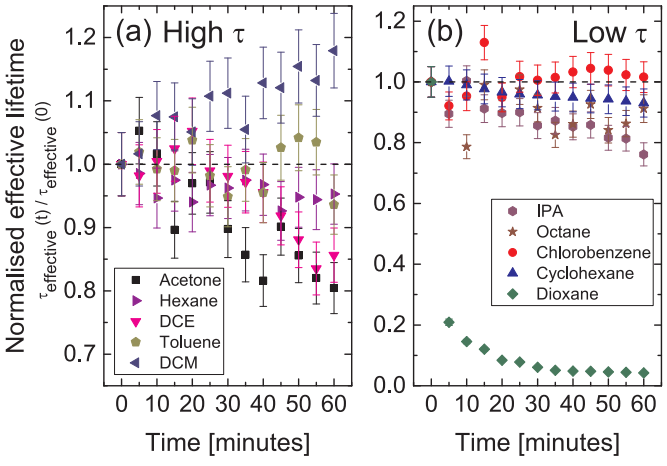

Fig. 2. Effective lifetime at an excess carrier density of 10^{15} cm^{-3} normalised by that of the first measurement versus time since first measurement for 5 Ω cm *n*-type float-zone silicon with a thickness of 750 μm samples passivated with TFSI dissolved in different solvents. Graph (a) shows results for the solvents which give high absolute lifetimes in Fig. 1, and graph (b) shows results for lower absolute lifetimes.

For the remainder of this paper we focus on TFSI-hexane based passivation.

3.3. Humidity effects on passivation

Experiments were conducted to establish the influence of storage humidity on the level of surface passivation achieved as a function of time. A single float-zone silicon wafer (5 Ω cm *n*-type) was cleaved into four quarter-wafer samples, which were all passivated with TFSI-hexane using the established method. The as-passivated lifetimes for the quarters were all in the interval 13.3 ± 0.1 ms, which demonstrates that the samples' initial states were identical within experimental error. After passivation, two samples were stored in ambient laboratory conditions (room relative humidity: 39 ± 2%); one with the 'lid off' the petri dish; another with its 'lid on'. The two other samples were stored in conditions deliberately engineered to deviate from ambient humidity. The "dry" sample was stored in a desiccator containing silica gel in which the relative humidity was measured to be below 20%. The "wet" sample was stored in a container with an open vessel of water, for which the relative humidity was measured to be above 70%. For lifetime measurements samples were removed from their low or high humidity environments for a short time (typically < 2 min for each measurement).

Fig. 3 shows that the temporal dependence of lifetime varies strongly according with the storage conditions. The key points are:

- The lifetime in the 'lid off' sample reduces considerably more rapidly than in the 'lid on' sample. The differences are considerable after 15 min and after ten hours the difference is approximately a factor of two.
- The sample kept in relatively dry conditions has a stable lifetime for the first half hour or so, but then starts to decay very rapidly until it reaches the lowest lifetime for any of the storage conditions.
- The sample stored in relatively wet conditions exhibits a sudden drop in lifetime in the first fifteen minutes and then decays relatively slowly ending up with a lifetime in between the two ambient samples.

Possible mechanisms for the differences in behaviour between the different storage conditions are discussed later.

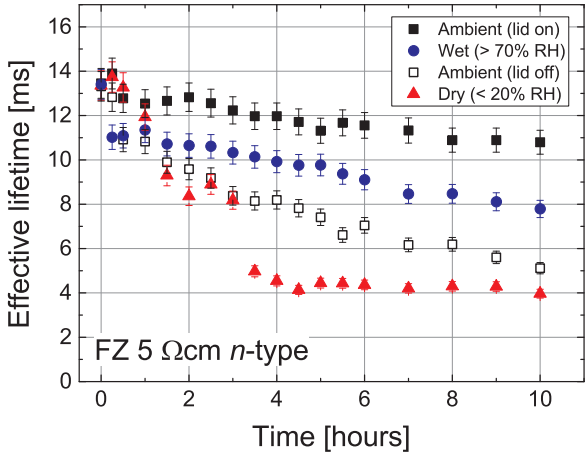

Fig. 3. The effect of humidity on effective lifetime at an excess carrier density of 10^{15} cm^{-3} for four quarters of a 5 Ω cm *n*-type float-zone silicon wafer. Samples were passivated with TFSI-hexane and were stored under the conditions indicated in the legend. Ambient relative humidity in the laboratory was 39 ± 2%, and the laboratory temperature was 24 ± 1 °C.

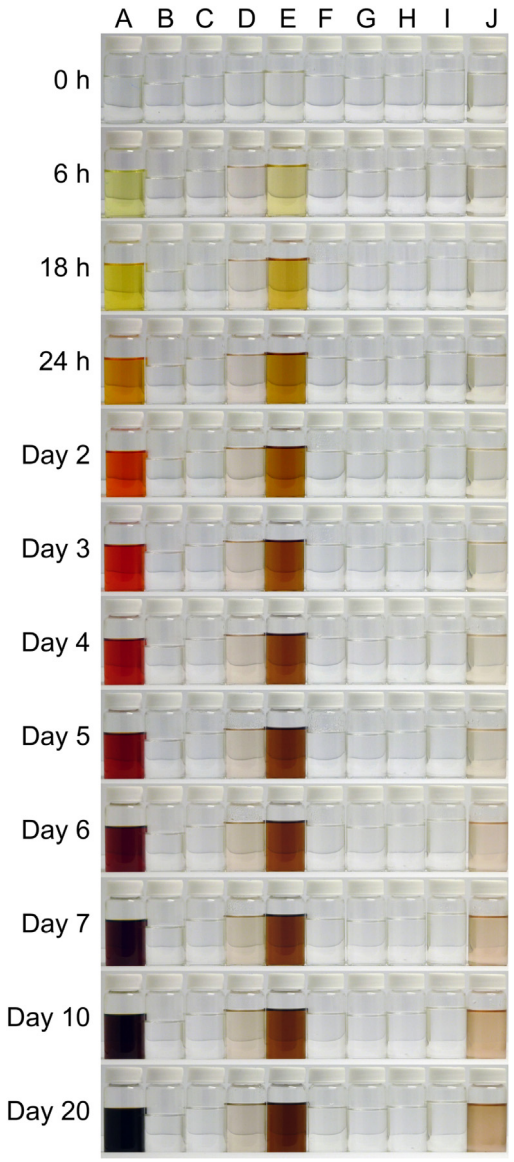

Fig. 4. Time series photographs showing vials containing solutions of TFSI in different solvents. The vials are labelled according to Table 1. Colour changes are observed for acetone (A), DCE (D), dioxane (E) and toluene (J).

3.4. Degradation of superacid-containing solutions

As well as the passivation quality degrading with time over timescale of a few hours, we have also found the age of the superacid-solvent solution to be an important factor in achieving the optimal passivation. Chemical reactions have been observed to occur in various TFSI-solvent systems, as evidenced by a colour change in the solution. Fig. 4 shows a time series of photographs of small sealed vials of various TFSI-solvent solutions. Colour changes are observed for acetone, DCE, dioxane and toluene even in the sealed vials depicted.

One of the main aims of this study is to find a replacement passivating solution for TFSI-DCE. The colours in Fig. 4 show that TFSI-DCE solutions undergo a chemical reaction in the absence of silicon and thus it seems likely that this chemical change may affect the quality of surface passivation. Even though TFSI-hexane, which emerged as the front-runner in Section 3.2, did not experience a noticeable colour change it is important to assess its long-term passivation ability. We therefore performed an experiment to passivate 5 Ωcm FZ silicon samples with new solutions and solutions which have been stored in air-tight bottles for 21 days. Results are presented in Fig. 5. After

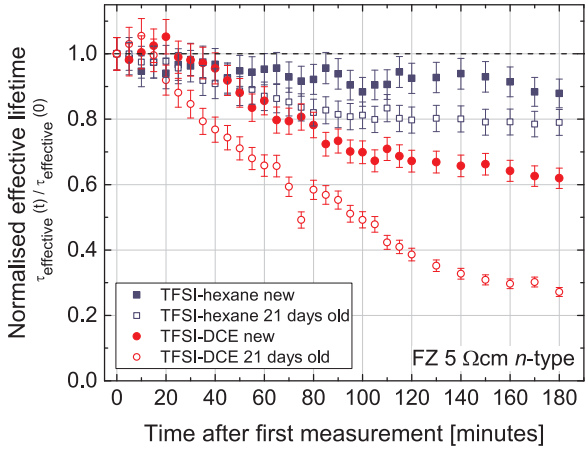

Fig. 5. A comparison of the time stability of TFSI-hexane and TFSI-DCE solutions in the fresh state and after 21 days of sealed storage. The effective lifetime at an excess carrier density of 10^{15} cm^{-3} at each time step was normalised by that of the first measurement.

passivation, these samples were stored in the dark in their petri dishes loosely covered by a lid between measurements. New solutions of TFSI-hexane and TFSI-DCE gave initially the same lifetimes within typical measurement errors [20]. These two solutions left for 21 days in sealed storage before application gave similarly high initial lifetimes, but degraded more strongly, particularly in the case of TFSI-DCE.

3.5. Extraction of bulk lifetime and effective surface recombination velocity

Having established the superiority of the passivation scheme arising from TFSI-hexane, a set of experiments was conducted to separate the contributions to effective lifetime arising from surface and bulk effects. For a symmetrically passivated lowly doped sample with relatively low surface recombination velocity, the injection-dependent effective lifetime, $\tau_{effective}$, varies according to:

$$\frac{1}{\tau_{effective}} = \frac{1}{\tau_{bulk}} + \frac{2S}{W} \quad (1)$$

where τ_{bulk} is the injection-dependent bulk lifetime, S is the injection-dependent effective surface recombination velocity, and W is the sample thickness. By measuring $\tau_{effective}$ in a set of samples with variable W and constant τ_{bulk} it is possible to determine both τ_{bulk} and S as a function of excess carrier density using Eq. (1).

A set of 3 Ω cm n-type FZ silicon wafers with different thicknesses were specially sourced from the same ingot for this experiment. These wafers were not cleaved and were measured whole to minimise edge effects. The wafers were passivated using the TFSI-hexane solution, and the best-case effective lifetime data are shown in Fig. 6(a). As expected, the effective lifetime increases with increasing wafer thickness due to the reducing influence of the surfaces. Our assumption is that τ_{bulk} is approximately the same in all these wafers, so any change in effective lifetime is due to differences in surface recombination. Fig. 6(b) shows plots in accordance with Eq. (1) used to extract S and τ_{bulk} at two different excess carrier densities. The fits to the data shown are very good with R^2 values of 0.978 and 0.990 at 10^{14} cm^{-3} and 10^{15} cm^{-3} injections, respectively. S is extracted as 0.68 ± 0.06 cms^{-1} and 0.69 ± 0.04 cms^{-1} for 10^{14} cm^{-3} and 10^{15} cm^{-3} injections, respectively, and τ_{bulk} is 41 ± 2 ms and 34 ± 2 ms, respectively. Eq. (1) is used at each level of averaged injection to extract the τ_{bulk} as a function of excess carrier density and this is also plotted in Fig. 6(a). Fig. 6(c) shows an uncalibrated photoluminescence image of the thinnest wafer characterised when 179 μm thick, which demonstrates the passivation is uniform across the wafer, and that there are no unusual bulk lifetime features in the samples studied, such as concentric ring-like features

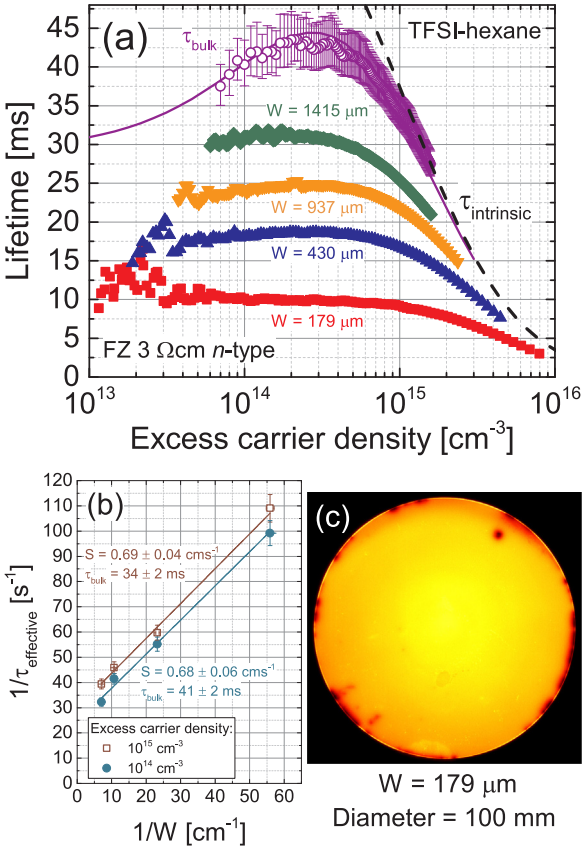

Fig. 6. (a) Effective lifetime measured in whole 100 mm diameter 3 Ω cm n-type FZ-Si wafers with different thicknesses from same ingot passivated with TFSI-hexane using the best case results (Test 4). Also shown are the current intrinsic lifetime limit [6] and the bulk lifetime extracted using Eq. (1) as a function of injection. (b) Plot used to extract surface recombination velocity and bulk lifetime from the data in (a). (c) Uncalibrated photoluminescence image of the passivated 179 μm thick 100 mm diameter wafer to show the uniformity.

which are sometimes observed in silicon lifetime images.

3.6. Reproducibility

An important issue for any temporary surface passivation scheme is the extent to which it is reproducible. A series of reproducibility tests was conducted using TFSI-hexane on the variable thickness 3 Ω cm n-type FZ silicon wafers from the same ingot. The tests are referred to as Tests 1–5, with Test 4 giving the best case results which have already been presented in Fig. 6. Fig. 7(a) shows the key results of the reproducibility experiments, with the reciprocal lifetime (at 10^{15} cm^{-3} injection) plotted as a function of the reciprocal wafer thickness according to Eq. (1). As each passivation step involved a chemical etch, it is noted that the samples become thinner each time they are tested.

One notable outlying point in Fig. 7(a) is Test 3 for the thickest sample tested (marked with an open green triangle), for which the lifetime is substantially lower than might be expected. The PL images shown in Fig. 7(b) shows why this is the case, with the centre of the wafer where the photoconductance lifetime measurement is made becoming damaged between Test 2 and Test 3, and recovering again for Test 4. PL images for other possible outliers in Fig. 7(a), such as Test 2 for the thinnest sample, were also inspected, but no significant marks were found in other cases. The possible origins of non-reproducibility are discussed later.

In a more detailed analysis, $1/\tau_{bulk}$ in Eq. (1) is fitted with Shockley-Read-Hall (SRH) theory, the Auger lifetime [6] and the radiative

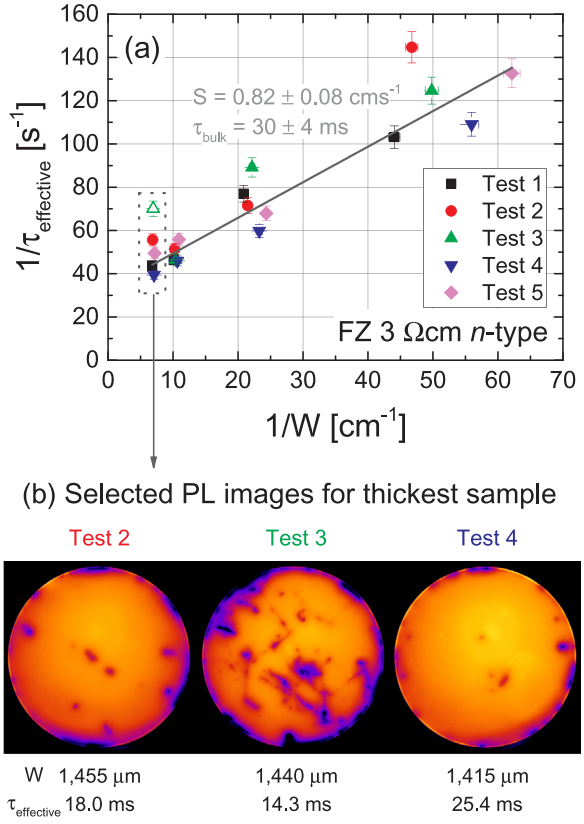

Fig. 7. Results of a reproducibility study on whole 100 mm diameter 3 Ω cm *n*-type FZ-Si wafers with different thicknesses from the same ingot passivated with TFSI-hexane. Lifetimes are extracted at 10^{15} cm^{-3} injection. (a) Plot in accordance with Eq. (1) to determine the effective surface recombination velocity and bulk lifetime. The open data point from Test 3 was excluded from the fit due to process-induced surface damage. (b) Selected uncalibrated PL images of the thickest sample for Tests 2–4, showing that surface damage during processing during Test 3 is removed by etching as part of Test 4.

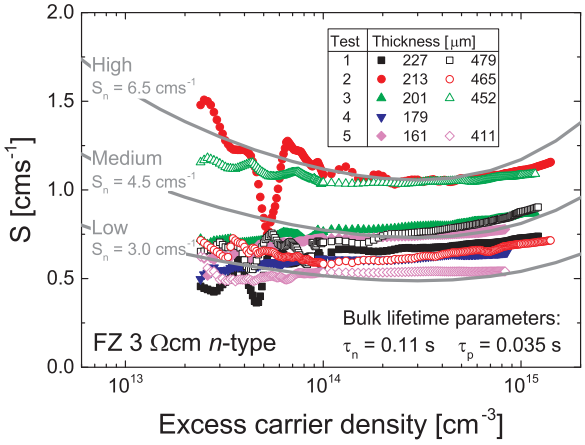

Fig. 8. Modelled effective surface recombination velocity (S) versus excess carrier density for whole 100 mm diameter 3 Ω cm *n*-type FZ-Si wafers from same ingot passivated with TFSI-hexane. Data are shown for the two thinnest wafers for Tests 1–5 (except Test 4 for the second thinnest sample) with the thinnest wafer being denoted with closed symbols and the next thinnest wafer denoted with open symbols. For these calculations $Q_f = -7 \times 10^{10}$ q cm^{-2} and three scenarios with different S_n values are shown, as described in the text.

lifetime [21,22] as $1/\tau_{SRH} + 1/\tau_{Auger} + 1/\tau_{radiative}$, in the whole measured injection range of Tests 1–5 and all wafer thicknesses. The overall residuals are smallest if the hole lifetime is chosen for all wafers as $\tau_p = 0.035$ s, but if τ_p is left free during the fitting procedure it only deviates by a small amount from 0.035 s. As the samples were not measured at injection densities exceeding about 2×10^{15} cm^{-3}, the electron lifetime, τ_n, does not influence the fitting result as much as τ_p with τ_n between 0.01 s and 0.02 s giving good fitting results with the defect energy in the mid gap. The two thinnest wafers are most sensitive to the surface passivation quality, and their resulting S values are plotted in Fig. 8. The analysis shown in Fig. 7(a) yielded $S = 0.82 \pm 0.08$ cm s^{-1} at an injection density of 1×10^{15} cm^{-3}, and this range indeed comprises about two thirds of all S values of Fig. 8, as is expected from Gaussian error analysis.

We fitted the S curves in Fig. 8 with Equation 3 of Ref. [23] and obtained the best fit near a fixed surface charge density of $Q_f = -7 \times 10^{10}$ q/cm^2 as denoted by the curves on the plot. The medium curve is obtained using a surface recombination velocity for electrons of $S_n = 4.5$ cm s^{-1}. The high and low curves have S_n values of 6.5 and 3 cm s^{-1}, respectively. For $Q_f > -6 \times 10^{10}$ q/cm^2, S increases sharply towards lower injection densities because no inversion is obtained anymore, while at $Q_f < -1 \times 10^{11}$ q/cm^2 and at positive Q_f values, S increases more pronouncedly at higher injection densities. We do not expect our fitting procedure to be a very reliable means to determine Q_f and therefore take $Q_f = -7 \times 10^{10}$ q/cm^2 as a mere indication. The negative value of Q_f is, however, also compatible with the decreasing lifetimes in Fig. 1 towards lower excess carrier densities.

4. Discussion

4.1. Level of surface passivation

In general surface passivation arises from two possible mechanisms, which are chemical passivation (i.e. termination of dangling bonds) and field effect passivation whereby carriers are repelled away from the surface by the presence of a charge. It is possible to relate the effective surface recombination velocity, S, to the unpassivated state density, N, according to $S = \sigma v_{th} N$, where σ is the capture cross-section and v_{th} is the thermal velocity of carriers. Taking a typical value of σ as 10^{-15} cm^2 and v_{th} as 10^7 cm s^{-1} with our best case S of around 0.7 cm s^{-1} for TFSI-hexane (Fig. 6), gives N as low as 7×10^7 cm^{-2}. This would be about 3–4 orders of magnitude lower than typical Al_2O_3, SiO_2 and Al_2O_3/SiN_x stack passivation [24–26]. However, this estimation assumes that there is zero interface charge and it is noted that for such low unpassivated state densities that a small amount of charge can have a huge impact on the level of surface passivation. Based on these assumptions, with our best passivation, the unpassivated dangling bonds would be separated by around 1.2 µm. Assuming $S_n = 4.5$ cm s^{-1} from the fitting procedure underpinning Fig. 8, gives N as 4.5×10^8 cm^{-2}, which is a separation of around 470 nm.

We do not consider it likely that the TFSI molecule itself passivates the silicon surface. Dangling bonds at the surface of silicon are separated by a lattice constant (5.431 Å) or less and the TFSI molecule is much larger than this and so is unlikely to give the ultra-low levels of unpassivated dangling bond densities we infer. Also, TFSI is likely to exist as a negatively charged anion which will be repelled away from any negatively charged dangling bonds. It seems most likely that the TFSI molecule breaks up and its constituents passivate the silicon surface, although it could still be possible that a large part of the molecule attaches itself to the surface vertically. Finally, it is noted that the effective surface recombination velocities achieved with TFSI-based passivation are similar to those achieved by HF immersion passivation, in which passivation is known to arise from hydrogen termination of dangling bonds [27]. It is however possible that other species (such as H or CF_3) are responsible for the passivation and this remains under investigation.

4.2. Solvent effects

Results presented in Fig. 1 and in the initial study by Bullock et al.

[10] show that the choice of solvent for TFSI can have a strong impact on the level of surface passivation achieved. Our work shows that there is no obvious correlation with the relative polarity of the solvent used (given in Table 1), with samples with high relative polarities (e.g. DCE, DCM) giving similar lifetimes to those with low relative polarities (e.g. hexane, toluene).

The mechanism by which the solvent influences the level of passivation is the subject of further study. There seems to be at least two ways in which it is possible for the solvent to affect the passivation. First, the solvent could be incorporated into the thin film which forms on the surface of the silicon. Second, the different solvents could change the pathway in which TFSI breaks apart and hence a variety of species could be responsible for the surface passivation in each case.

In general, passivation achieved with TFSI dissolved in oxygen-containing solvents (acetone, dioxane and IPA) degrades faster than with oxygen-free solvents (Fig. 2). It could be the case that the solvent, or some of its constituent atoms, are contained in the thin film which forms on the silicon surface, or it could be that the TFSI molecule breaks up via specific routes depending on how it binds to the solvent. Furthermore, the injection dependence with acetone is different to the other solvents and is similar to that observed for acetonitrile (relative polarity 0.460 [19]) in the work of Bullock et al. [10]. These solvents contain oxygen and nitrogen, respectively, and so it is possible that these atoms are incorporated into the passivating thin film or influence the TFSI break up in some way. The different injection dependences suggest that the films which form with acetone and acetonitrile have different in-built charge densities to the other films, and this therefore could result in a field effect modifying the effective surface passivation.

The colour changes observed in Fig. 4 are evidence of reactions happening between the solvent and TFSI and this is not surprising given the plethora of acid catalysed organic reactions that exist. In the simplest case with acetone, it is likely that self-condensation or cross-condensation [28] has occurred here. Further to this, recent studies have shown that more complex reactions can take place when DCE [29] and toluene [30,31] react with a variety of superacids. Characterisation of these solutions would need to be done to identify the products created and these solvents are probably unsuitable for passivation of silicon as these side reactions may hinder the passivation mechanism. Moreover, to ensure the passivation would be reproducible, a new solution would have to be made each time and this would be wasteful and expensive.

The solution aging results (Fig. 5) indicate that better results are achieved with new solutions for both TFSI-DCE and TFSI-hexane. Both new solutions initially provide similar levels of surface passivation, however after ~1 h, there is a distinct deviation between the two. This would only occur if the films slightly differ in either their composition or charge state, which stem directly from the solvent, as this is the only variable. We thus infer that the solvent plays a role in both the passivation level and stability of the film, and this is supported by Fig. 1. It could be that the degradation rate is determined by water moisture contamination of the passivating solutions. At 25 °C the solubility of water in DCE is 0.1262 M [32], whereas in hexane it has a much lower value of 0.00362 M [33]. This could mean more water would be incorporated into the film in the DCE case and so this could explain differences. For 21 day old solutions, TFSI-DCE is much worse than a new solution, while the passivation arising from the old TFSI-hexane solution shows only slightly worse degradation than its new solution. From Fig. 4, it is evident that TFSI-DCE undergoes some self-reaction and this could explain the increased degradation with the older solution.

4.3. Atmospheric humidity issues

The results shown in Fig. 3 show that the surface passivation degradation behaviour of TFSI-hexane is dependent on the conditions under which the sample is stored. Setting aside the ambient lid on case initially, the wet, ambient lid off and dry cases occur in order of decreasing relative humidity (> 70%, 39% and < 20%, respectively), and their passivation degradation rates are also in order with the least degradation occurring in the most humid case. This therefore suggests that the presence of some moisture in the environment is beneficial for retaining the surface passivation effect. In a dry environment there is a driving force for evaporation from the passivating film and the removal of moisture from the film – whose composition is as yet unknown – could reduce the level of passivation. It is noted that the dry case in Fig. 3 appears to plateau after 4 h. This could be due to equilibrium being established between the film and environment, which would appear to support the idea of drying out of the passivating film. In a wet environment there is less of a driving force for evaporation from the passivating film and it might even be that water from the environment becomes absorbed into the passivating film, effectively diluting the chemical passivation effect. This dilution effect is supported by the TFSI-DCE study of Bullock et al. who found adding water to the passivating solution decreases the level of surface passivation [10].

The most stable behaviour is achieved under normal laboratory conditions with the lid kept on the sample. In this case the local environment beneath the lid and the passivation film can be approximated as a closed system. No additional water can access the film to dilute the passivation. Any degradation which does occur in the lid on sample could occur when the lid is removed for lifetime measurement purposes and also could be due to any leaks which occur due to the relatively loose attachment of the lid. More experimental work is currently underway to understand the humidity effects further, which will only be fully understood when the detailed chemical compositions of the films are known.

4.4. Measurement of long lifetimes

Various studies have recently measured or inferred bulk lifetimes exceeding the Richter et al. intrinsic so-called limit [6]. Many are in *n*-type silicon and are for resistivities of 0.47 Ω cm [1], 1 Ωcm [2,4,5] and 1.4 Ω cm [3]. The methodology used in this paper based on using variable thickness wafers from the same ingot is rarely used in passivation studies. As such, we believe our results in Fig. 6 are extremely robust. We do not exceed the limit of Richter et al. with 3 Ω cm *n*-type material, so our study provides no evidence for the existing intrinsic limit being conservative at this resistivity. The methodology used here, with variable thickness wafers from the same ingot, would provide an excellent way of re-parameterising the intrinsic lifetime limit of silicon for low resistivity material, but currently no suitable sample set is available to us.

4.5. Using superacid-derived surface passivation for reproducible characterisation in process development

The TFSI-DCE passivation scheme developed in previous studies [2,10] has been demonstrated to be effective at understanding the origin of efficiency degradation of IBC cells [11] and also for separating bulk and surface passivation effects in light induced degradation investigations [34,35]. However, the work presented in this paper has shown TFSI-hexane to be superior to TFSI-DCE in many ways, including giving marginally higher lifetimes (Fig. 1), better passivation stability over 1–3 h (Figs. 2 and 5), and better solution longevity (Fig. 5). TFSI-DCE has been observed to undergo a colour change suggesting a reaction is occurring in the solution (Fig. 4). These factors, combined with the knowledge that DCE is “possibly carcinogenic to humans” [12], means that we now advocate the use of TFSI-hexane for the purposes of measuring high bulk lifetimes.

Regardless of the choice of superacid-containing passivation solution, there are many subtleties which need to be understood to use such a passivation scheme in cell process development. In setting up such a passivation scheme it is first important to realise that substantial differences in bulk lifetime can occur in as-received wafers (even high

purity FZ ones). We have previously shown substantial wafer-to-wafer variation can be found within a box of wafers from the same supplier [16]. To use this, or any other, passivation technique in high lifetime process development it is therefore usually necessary to subject all wafers to a pre-anneal to homogenise the lifetime. A high temperature pre-anneal at approximately 1000 °C usually prevents the re-formation of defects later during future cell processes [15,16], and a low temperature anneal at about 200 °C [14] (as used for the results presented in Figs. 6 and 7) can annihilate recombination centres temporarily with the risk that they will be re-formed during subsequent thermal processing. We have found that the lower temperature anneal is a practical solution in the laboratory as it does not need to be performed in very clean conditions.

We have shown that superacid-derived passivation can be used reasonably reproducibly, but, as with any passivation scheme (including dielectric layers deposited by plasma enhanced chemical vapour deposition or atomic layer deposition), minor problems with surface preparation can strongly influence the results achieved. We note that in Fig. 7(b) the thickest sample became damaged at some point between Test 2 and Test 3. The photoconductance lifetime measured in this sample was still very high (14.3 ms), but the PL imaging reveals scratches in the central area of the wafer, which we believe are very shallow and are introduced during handling of the whole wafer during the HF dip stage immediately prior to passivation. Other points in Fig. 7(a), such as Test 2 for the thinnest sample, show deviation from the expected trend but no damage was found in the PL images (not shown). In this case we suspect the variation arose due to a minor issue with the cleaning procedure. The best results were achieved in Test 4 for which a brand new TMAH solution was used, but this may be coincidental.

5. Conclusions

A systematic study was performed into the surface passivation of *n*-type silicon samples treated with TFSI solutions made with various anhydrous solvents. All solutions investigated passivated the surface to some extent, and the passivation quality was not found to correlate with the relative polarity of the solvent. Excellent initial surface passivation was achieved with several solvents, including hexane, DCE, toluene and DCM. TFSI solutions made with DCE and toluene are however unstable as evidenced by colour changes, and, whilst DCM gives good results, the use of a chlorinated solvent is undesirable. TFSI-hexane gives better surface passivation than TFSI-DCE used previously and provides better passivation stability and solution longevity. Hexane is also arguably safer than DCE, which is possibly carcinogenic, so it is concluded that TFSI-hexane is a better solution to use for superacid immersion passivation of silicon than TFSI-DCE used previously.

A series of investigations was performed into the TFSI-hexane passivation scheme. The stability of the passivation was strongly influenced by the storage humidity of the sample after passivation. The passivation was most stable when the samples are kept in a petri dish with the lid on. Further investigations are required to understand the composition of the passivating thin films on the silicon surface. TFSI-hexane passivation was applied to a set of FZ silicon wafers cut with different thicknesses from the same ingot. This enabled the extraction of the bulk lifetime and surface recombination velocity. The best case effective surface recombination velocity was $0.69 \pm 0.04\,\mathrm{cm\,s^{-1}}$. A series of five tests was performed on the same sample set, thus demonstrating the reproducibility of the scheme.

In summary, a superacid immersion treatment has been developed which consistently provides a very low surface recombination velocity with minimal test-to-test variation. This is an important step towards giving researchers the ability to determine the bulk lifetime accurately with good reliability and to ascertain the surface passivation quality of their desired passivation schemes, especially as cell efficiencies become more sensitive to surface and bulk recombination effects.

Acknowledgments and data access statement

This work was supported by the EPSRC SuperSilicon PV project (EP/M024911/1). A.I. Pointon was supported by an EPSRC Doctoral Studentship (EP/N509796/1) and E.C. Wheeler-Jones was partially supported by the EPSRC Centre for Doctoral Training in Molecular Analytical Science (EP/L015307/1). Sune Bro Duun of Topsil Semiconductor Materials is gratefully acknowledged for provision of the FZ-Si wafers with variable thickness from the same ingot. Data published in this article can be freely downloaded from http://wrap.warwick.ac.uk/99904.

Declarations of interest

None.

Appendix A. Supplementary material

Supplementary data associated with this article can be found in the online version at http://dx.doi.org/10.1016/j.solmat.2018.03.028.

References

[1] Y. Wan, K.R. McIntosh, A.F. Thomson, A. Cuevas, "Low surface recombination velocity by low-absorption silicon nitride on c-Si". *Proceedings of the 38th IEEE Photovoltaic Specialists Conference (PVSC)* (Austin, TX, USA), doi: 10.1109/PVSC-Vol2.2013.6656792, 2012.

[2] N.E. Grant, T. Niewelt, N.R. Wilson, E.C. Wheeler-Jones, J. Bullock, M. Al-Amin, M.C. Schubert, A.C. van Veen, A. Javey, J.D. Murphy, Superacid-treated silicon surfaces: extending the limit of carrier lifetime for photovoltaic applications, IEEE J. Photovolt. 7 (2017) 1574, http://dx.doi.org/10.1109/JPHOTOV.2017.2751511.

[3] B.A. Veith-Wolf, J. Schmidt, Unexpectedly high minority-carrier lifetimes exceeding 20 ms measured on 1.4-Ω cm n-type silicon wafers, Phys. Status Solidi Rapid Res. Lett. 11 (2017) 1700235, http://dx.doi.org/10.1002/pssr.201700235.

[4] T. Niewelt, W. Kwapil, M. Selinger, A. Richter, M.C. Schubert, Long-term stability of aluminum oxide based surface passivation schemes under illumination at elevated temperatures, IEEE J. Photovolt. 7 (2017) 1197, http://dx.doi.org/10.1109/JPHOTOV.2017.2713411.

[5] R.S. Bonilla, C. Reichel, M. Hermle, P.R. Wilshaw, Extremely low surface recombination in 1 Ω cm n-type monocrystalline silicon, Phys. Status Solidi Rapid Res. Lett. 11 (2017) 1600307, http://dx.doi.org/10.1002/pssr.201600307.

[6] A. Richter, S.W. Glunz, F. Werner, J. Schmidt, A. Cuevas, Improved quantitative description of Auger recombination in crystalline silicon, Phys. Rev. B 86 (2012) 165202, http://dx.doi.org/10.1103/PhysRevB.86.165202.

[7] R.S. Bonilla, B. Hoex, P. Hamer, P.R. Wilshaw, Dielectric surface passivation for silicon solar cells: a review, Phys. Status Solidi A 214 (2017) 1700293, http://dx.doi.org/10.1002/pssa.201700293.

[8] A.Y. Liu, C. Sun, V.P. Markevich, A.R. Peaker, J.D. Murphy, D. Macdonald, Gettering of interstitial iron in silicon by plasma-enhanced chemical vapour deposited silicon nitride films, J. Appl. Phys. 120 (2016) 193103, http://dx.doi.org/10.1063/1.4967914.

[9] N.E. Grant, J.D. Murphy, Temporary surface passivation for characterisation of bulk defects in silicon: a review, Phys. Status Solidi Rapid Res. Lett. 11 (2017) 1700243, http://dx.doi.org/10.1002/pssr.201700243.

[10] J. Bullock, D. Kiriya, N. Grant, A. Azcatl, M. Hettick, T. Kho, P. Phang, H.C. Sio, D. Yan, D. Macdonald, M.A. Quevedo-Lopez, R.M. Wallace, A. Cuevas, A. Javey, Superacid passivation of crystalline silicon surfaces, ACS Appl. Mater. Interfaces 8 (2016) 24205, http://dx.doi.org/10.1021/acsami.6b07822.

[11] T. Rahman, A. To, M.E. Pollard, N.E. Grant, J. Colwell, D.N.R. Payne, J.D. Murphy, D.M. Bagnall, B. Hoex, S.A. Boden, Minimising bulk lifetime degradation during the processing of interdigitated back contact silicon solar cells, Prog. Photovolt.: Res. Appl. 26 (2018) 38, http://dx.doi.org/10.1002/pip.2928.

[12] 1,*2-Dichloroethane*. IARC Monographs on the Evaluation of Carcinogenic Risks to Humans (Lyon, France), 71, 1999, p. 501.

[13] J.-W. Song, C.C. Nguyen, S.-W. Song, Stabilized cycling performance of silicon oxide anode in ionic liquid electrolyte for rechargeable lithium batteries, RSC Adv. 2 (2012) 2003, http://dx.doi.org/10.1039/c2ra01183b.

[14] N.E. Grant, F.E. Rougieux, D. Macdonald, J. Bullock, Y. Wan, Grown-in defects limiting the bulk lifetime of p-type float-zone silicon wafers, J. Appl. Phys. 117 (2015) 055711, http://dx.doi.org/10.1063/1.4907804.

[15] N.E. Grant, V.P. Markevich, J. Mullins, A.R. Peaker, F. Rougieux, D. Macdonald, Thermal activation and deactivation of grown-in defects limiting the lifetime of float-zone silicon, Phys. Status Solidi Rapid Res. Lett. 10 (2016) 443, http://dx.doi.org/10.1002/pssr.201600080.

[16] N.E. Grant, V.P. Markevich, J. Mullins, A.R. Peaker, F. Rougieux, D. Macdonald, J.D. Murphy, Permanent annihilation of thermally activated defects which limit the lifetime of float-zone silicon, Phys. Status Solidi A 213 (2016) 2844, http://dx.doi.org/10.1002/pssa.201600360.

[17] M. Kessler, T. Ohrdes, P.P. Altermatt, R. Brendel, The effect of sample edge

recombination on the averaged injection-dependent carrier lifetime in silicon, J. Appl. Phys. 111 (2012) 054508, http://dx.doi.org/10.1063/1.3691230.
[18] B. Veith, T. Ohrdes, F. Werner, R. Brendel, P.P. Altermatt, N.-P. Harder, J. Schmidt, Injection dependence of the effective lifetime of *n*-type Si passivated by Al_2O_3: an edge effect? Sol. Energy Mater. Sol. Cells 120 (2014) 436, http://dx.doi.org/10.1016/j.solmat.2013.06.049.
[19] C. Reichardt, T. Welton, Solvent and Solvent Effects in Organic Chemistry, 4th ed., Wiley-VCH, 2011.
[20] A.L. Blum, J.S. Swirhun, R.A. Sinton, F. Yan, S. Herasimenka, T. Roth, K. Lauer, J. Haunschild, B. Lim, K. Bothe, Z. Hameiri, B. Seipel, R. Xiong, M. Dhamrin, J.D. Murphy, Inter-laboratory study of eddy-current measurement of excess-carrier recombination lifetime, IEEE J. Photovolt. 4 (2014) 525, http://dx.doi.org/10.1109/JPHOTOV.2013.2284375.
[21] T. Trupke, M.A. Green, P. Würfel, P.P. Altermatt, A. Wang, J. Zhao, R. Corkish, Temperature dependence of the radiative recombination coefficient of intrinsic crystalline silicon, J. Appl. Phys. 94 (2003) 4930, http://dx.doi.org/10.1063/1.1610231.
[22] P.P. Altermatt, F. Geelhaar, T. Trupke, X. Dai, A. Neisser, E. Daub, Injection dependence of spontaneous radiative recombination in crystalline silicon: experimental verification and theoretical analysis, Appl. Phys. Lett. 88 (2006) 261901, http://dx.doi.org/10.1063/1.2218041.
[23] S. Steingrube, P.P. Altermatt, D.S. Steingrube, J. Schmidt, R. Brendel, Interpretation of recombination at c-Si/SiN_x interfaces by surface damage, J. Appl. Phys. 108 (2010) 014506, http://dx.doi.org/10.1063/1.3437643.
[24] J. Albohn, W. Füssel, N.D. Sinh, K. Kliefoth, W. Fuhs, Capture cross sections of defect states at the Si/SiO_2 interface, J. Appl. Phys. 88 (2000) 842, http://dx.doi.org/10.1063/1.373746.
[25] L.E. Black, T. Allen, K.R. McIntosh, A. Cuevas, Effect of boron concentration on recombination at the p-Si–Al_2O_3 interface, J. Appl. Phys. 115 (2014) 093707, http://dx.doi.org/10.1063/1.4867643.
[26] D. Schuldis, A. Richter, J. Benick, P. Saint-Cast, M. Hermle, S.W. Glunz, Properties of the c-Si/Al_2O_3 interface of ultrathin atomic layer deposited Al_2O_3 layers capped by SiN_x for c-Si surface passivation, Appl. Phys. Lett. 105 (2014) 231601, http://dx.doi.org/10.1063/1.4903483.
[27] E. Yablonovitch, D.L. Allara, C.C. Chang, T. Gmitter, T.B. Bright, Unusually low surface-recombination velocity on silicon and germanium surfaces, Phys. Rev. Lett. 57 (1986) 249, http://dx.doi.org/10.1103/PhysRevLett.57.249.
[28] G.S. Salvapati, K.V. Ramanamurty, M. Janardanarao, Selective catalytic self-condensation of acetone, J. Mol. Catal. 54 (1989) 9, http://dx.doi.org/10.1016/0304-5102(89)80134-8.
[29] T. Boudewijns, M. Piccinini, P. Degraeve, A. Liebens, D. De Vos, Pathway to vinyl chloride production via dehydrochlorination of 1,2-dichloroethane in ionic liquid media, ACS Catal. 5 (2015), p. 4043, http://dx.doi.org/10.1021/acscatal.5b00736.
[30] B.-Q. Xu, D. Sood, A.V. Iretskii, M.G. White, Direct Synthesis of dimethylbiphenyls by toluene coupling in the presence of palladium triflate and triflic acid, J. Catal. 187 (1999) 358, http://dx.doi.org/10.1006/jcat.1999.2616.
[31] S.C. Sherman, A.V. Iretskii, M.G. White, C. Gumienny, L.M. Tolbert, D.A. Schiraldi, Isomerization of substituted biphenyls by superacid. a remarkable confluence of experiment and theory, J. Org. Chem. 67 (2002) 2034, http://dx.doi.org/10.1021/jo0106445.
[32] J.R. Johnson, S.D. Christian, H.E. Affsprung, The molecular complexity of water in organic solvents. Part II, J. Chem. Soc. A: Inorg. Phys. Theor. 1966 (77) (1966), http://dx.doi.org/10.1039/J19660000077.
[33] J.W. Roddy, C.F. Coleman, Solubility of water in hydrocarbons as a function of water activity, Talanta 15 (1968) 1281, http://dx.doi.org/10.1016/0039-9140(68)80050-5.
[34] T. Niewelt, M. Selinger, N.E. Grant, W.M. Kwapil, J.D. Murphy, M.C. Schubert, Light-induced activation and deactivation of bulk defects in boron-doped float-zone silicon, J. Appl. Phys. 121 (2017) 185702, http://dx.doi.org/10.1063/1.4983024.
[35] D. Sperber, A. Graf, D. Skorka, A. Herguth, G. Hahn, Degradation of surface passivation on crystalline silicon and its impact on light-induced degradation experiments, IEEE J. Photovolt. 7 (2017) 1627, http://dx.doi.org/10.1109/JPHOTOV.2017.2755072.